This article has been accepted for publication in a future issue of this journal, but has not been fully edited. Content may change prior to final publication. Citation information: DOI 10.1109/TMAG.2015.2433394, IEEE Transactions on Magnetics

Magnetic Interaction and Electronic Transport in $La_{0.4}Bi_{0.6}Mn_{0.5}Ti_{0.5}O_3$ Manganite

Vijaylakshmi Dayal[1#], Punith Kumar V.[1], R. L. Hadimani[2], E. A. Balfour[3], H. Fu[3] and D. C. Jiles[2]

[1]Department of Physics, Maharaja Institute of Technology-Mysore, Karnataka 571438, India
[2]Department of Electrical and Computer Engineering, Iowa State University, Ames, IA 50011, USA
[3]School of Physical Electronics, University of Electronic Science and Technology of China, 610054, People's Republic of China

***Abstract*—We report magnetic interactions and electronic transport properties in $La_{0.4}Bi_{0.6}Mn_{0.5}Ti_{0.5}O_3$ perovskite manganite synthesized using solid state route. After characterizing the samples structurally, systematic investigations of magnetic and electrical transport behaviors have been undertaken. It has been observed that at low temperatures near T_C, the sample is magnetically frustrated leading to second order magnetic transition. A justification for the observed magnetic behaviour has been explained based on Arrott's plot study. The resistivity as a function of temperature in the absence and presence of applied magnetic field suggests semiconducting nature of the sample. The conduction of the charge carriers is explained using Shklovskii–Efros-type variable range hopping mechanism.**

***Index Terms* - Perovskite manganite; Magnetic properties; Arrott Plots; SE-VRH mechanism; Hopping conduction.**

I. Introduction

IN recent years perovskite type manganites with general formula ABO_3 have attracted significant deliberation because of their importance both for potential magnetoelectronic (ME) applications and fundamental research in condensed matter physics [1, 2]. The properties of these materials such as magnetoresistance (MR %), metal-insulator (M-I) transition, charge and magnetic ordering etc. have attracted significant attention [2]. The substitution of divalent or other trivalent rare earth ions at A-site results in varying the average cationic radii, introducing changes in bond angles and bond lengths. However, the B-site substitution induces local disorder directly into the Mn-O network significantly affecting their magnetism and conductivity [3, 4, 5].

In this paper, we present a study on the nature of the magnetic interactions near the magnetic transition and electronic-transport in a polycrystalline $La_{0.4}Bi_{0.6}Mn_{0.5}Ti_{0.5}O_3$. The substitution of non-rare earth ion such as Bi^{3+} (1.24Å) having ionic radii close to La^{3+}(1.22Å), has attracted much attention due to their potential application as lead-free magneto-electronic (ME) materials [1, 5]. The presence of the $6S^2$ lone pair of Bi^{3+} leads to the appreciable ME effects and ferro/antiferromagnetic ordering has been anticipated due to the coupling of the transition metal cation spins. Non-magnetic ions like Ti as a substitute at B site is particularly interesting in order to improve ME behavior [5].

II. Experimental Procedure

Polycrystalline $La_{0.4}Bi_{0.6}Mn_{0.5}Ti_{0.5}O_3$ perovskite manganite has been synthesized using conventional solid state reaction method [5]. High purity powder oxides La_2O_3 (99.99 %), Bi_2O_3 (99.9 %), MnO_2 (99.9 %) and TiO_2 (99.9 %) (Sigma Aldrich & Co) weighed in stoichiometric ratios have been used in sample synthesis. Due to volatile nature of Bi, we have followed low temperature synthesis procedure for the formation of perovskite structure. The phase purity has been verified by X-ray diffraction (XRD) using Cobalt source at room temperature. The field emission scanning electron microscope (FE-SEM) spectrometer equipped with Electron dispersion X-ray spectroscopy (EDS) has been used for the microscopic and elemental compositional analysis. Electrical resistivity measurements as a function of temperature and magnetic field have been carried out using standard four probe setup. For in-field measurements magnetic field has been applied parallel to the direction of current, built-in with Oxford spectromag 10T superconducting magnet at University Grant Commission-Department of Atomic Energy, Consortium for Scientific Research (UGC-DAE CSR), Indore. DC magnetization as a function of magnetic field and temperature were carried out using Superconducting Quantum Interference Device-Magnetic Properties Measurements Systems (Quantum Design SQUID- MPMS XL 5).

Manuscript received April 23, 2015 (date on which paper was resubmitted for review). Corresponding author: #**Dr. Vijaylakshmi Dayal** (e-mail: drvldayal@gmail.com, Mobile No. 09620228132).
Digital Object Identifier inserted by IEEE

III. Results and Discussions

Fig. 1 shows the low intense X-Ray Diffraction (XRD) pattern of the sample with small amount (<10%) of un-reacted Bi_2O_3 impurity peaks which arises due to the low temperature synthesizing process.

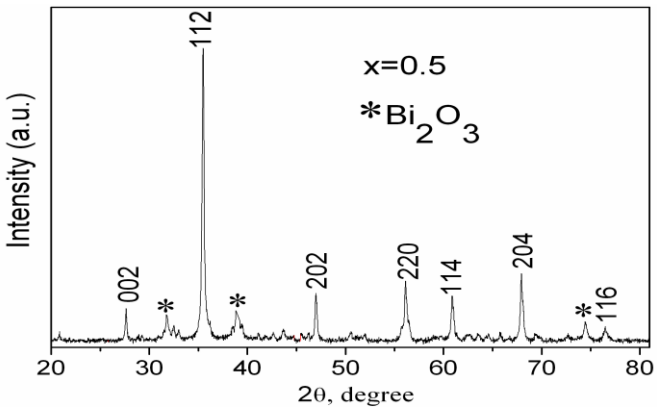

Fig. 1 display XRD pattern for the studied sample. Asterisk is impurity peaks due to un-reacted Bi_2O_3.

This article has been accepted for publication in a future issue of this journal, but has not been fully edited. Content may change prior to final publication. Citation information: DOI 10.1109/TMAG.2015.2433394, IEEE Transactions on Magnetics

The Rietveld refinement on the XRD pattern yields tetragonal perovskites structure indexed using I4/mcm space group. The lattice parameters have been found to be, a= 5.432 Å, b= 5.432 Å and c=7.716 Å with cell volume V=227.67 Å^3.

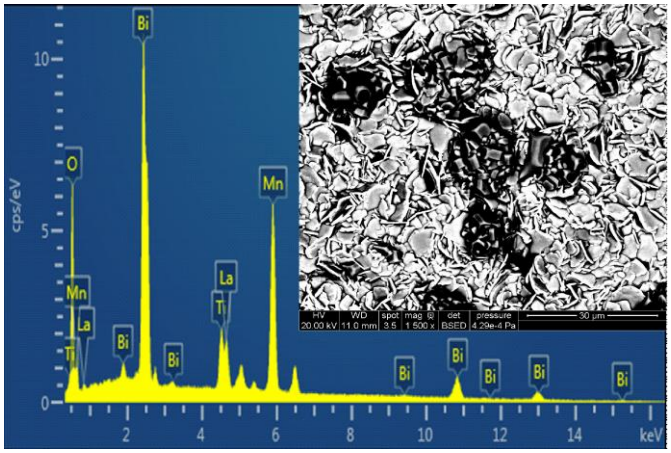

Fig. 2 EDS pattern of the sample. Inset of the figure we show magnified FE-SEM image at 30μm resolution.

In Fig. 2 EDS pattern shows the presence of elements in the sample close to their chemical compositions. Inset of Fig.2 we show micro-structural morphology of the studied sample using FE-SEM. The grains show distinct shape with well-defined grain boundaries. But the uniformity of the grain shapes is non homogeneous and also form agglomeration (dark patches) attributed due to the strain produced by Ti ions on the lattice arrangements [6, 7] or may be due to visco-elastic character of the sintered samples.

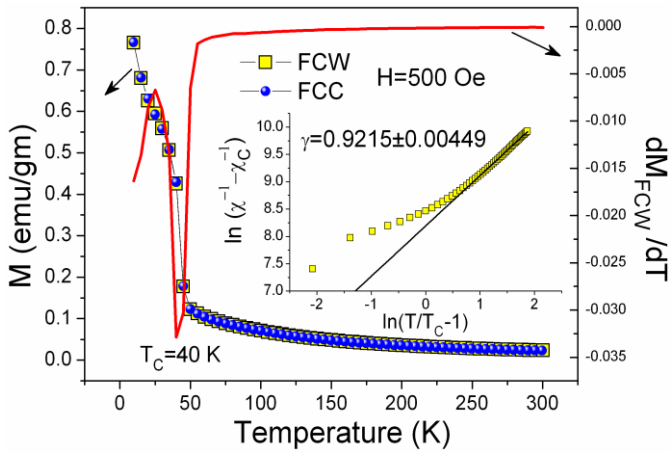

Fig. 3 displays M (emu/gm) vs. T (K) for the sample at H=500 Oe (left side) dM$_{FCW}$/dT (right side). Inset ln (χ^{-1}- χ_C^{-1}) vs. ln (T/T$_C$-1) for the sample at H=500 Oe. Solid line is fit to the experimental data.

In Fig. 3 we show MT plot at constant magnetic field H=500 Oe measured both in field cooled cooling (FCC) and field cooled warming (FCW) conditions. The MT plot doesn't show thermal hysteresis between FCC and FCW which confirms the paramagnetic (PM) to frustrated ferromagnetic (FM) phase transition at T$_C$=40 K is of second order type. The magnetic T$_C$ is obtained from dM$_{FCW}$/dT plot as shown in Fig. 3. The unsaturated FM behavior at low temperature indicates critical behavior around T$_C$ arising due to magnetic inhomogenities of Ti substitution [5].

In order to understand this critical nature we have analyzed the DC susceptibility obtained from MT plot using critical scaling hypothesis. While approaching magnetic transition temperature, T$_C$ from the PM side, DC susceptibility, χ (T) is expected to follow the scaling law [8] given as χ (T) ~ (T/T$_C$-1)$^{\gamma} \equiv \tau^{\gamma}$. The scaling equation is modified accordingly as, χ^{-1}-$\chi_C^{-1} \approx \tau^{\gamma}$, where $\chi_C = \chi(T_C)$, τ = T/T$_C$−1 and γ is critical exponent. The plot of ln (χ^{-1}- χ_C^{-1}) vs. ln (T/T$_C$−1) is shown in inset of Fig.3 for the studied sample. Linear fitting the above plot yields the value of slope (γ) =0.92 which deviates from unity suggesting that the sample doesn't possess long range FM interaction below T$_C$.

In Fig. 4 we show magnetization (M) vs. magnetic field (H) isotherms measured in the temperature (T) range of 10≤ T≤ 60 K exhibits critical behavior around T$_C$. At 10 K, magnetization rises sharply with the increase in applied magnetic field and shows no evidence of saturation up to 5T. The linear variation of M vs. H at high field as expected for an antiferromagnet (AFM) can be observed for other measured temperatures also, which implies that the compound exhibits magnetic frustration near T$_C$. The closer magnetization measurements in the temperature range 30-40K have been carried up to 2.5 T, which also shows no evidence of saturation. And at 300K the sample shows proper PM nature.

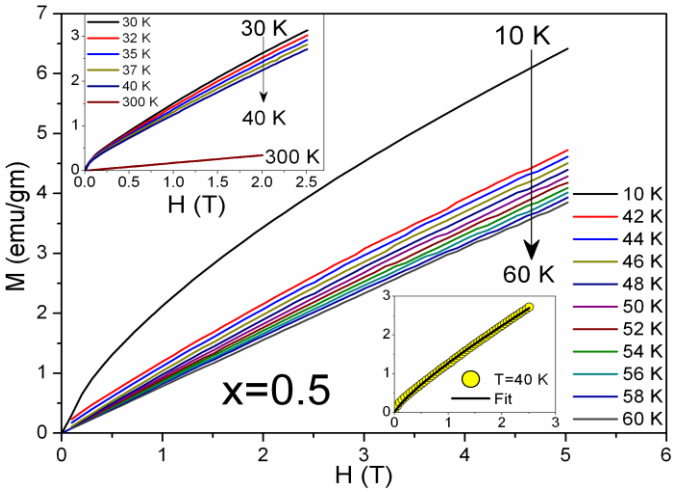

Fig. 4 displays MH isotherms for the sample at constant temperatures. Inset MH isotherms at constant temperatures measured up to 2.5T. In below inset the MH data at T=40 K with experimental fitting is displayed.

Further we have fitted the M-H isotherm to understand the magnetic interaction at T$_C$=40 K (inset of Fig.4) using critical scaling equation, $M=DH^{1/\delta}$ [9], where D is critical amplitude and δ is critical magnetization exponent. The best fit value of δ obtained using above equation is found to be ~2.0. This is less than the value of 3 (for ideal long range) further confirms the absence of long range FM interaction around T$_C$ [9].

This nature of absence of long range FM interactions around magnetic T$_C$ likely leads to a phenomenon called Griffith's phase [4, 10]. This is shown by the evidence of the downturn deviation from the characteristic Curie–Weiss linear law and

This article has been accepted for publication in a future issue of this journal, but has not been fully edited. Content may change prior to final publication. Citation information: DOI 10.1109/TMAG.2015.2433394, IEEE Transactions on Magnetics

the formation of FM clusters embedded in host PM matrix which is already been reported by us for the aforesaid and similar kind of sample [4, 10].

The regular Arrott plot shown in Fig. 5 as $M^{1/\beta}$ vs. $(H/M)^{\gamma}$ relationship is based on the mean-field (MF) model of critical exponent $\beta = 0.5$ and $\gamma = 1.0$. Thus M^2 vs. H/M curves reveal the magnetic nature around T_C and the extrapolation of the fitted line on magnetization data at $T = T_C$ should pass through the origin. According to the criterion proposed by *Banerjee et al.* [11], the order of magnetic transition can be determined from the slope of these straight lines. In the present study, the Arrott plot M^2 vs. H/M displays the positive slope of the curves at all temperatures studied. This specifies that a transition between the magnetically ordered and the PM phases is of the second order. The critical temperature of magnetic transition could not be evaluated from Arrott plots as the high magnetic field plot extrapolation did not reach origin. This suggested that the competition amongst the FM and AFM interactions lead magnetic transition is spread broadly both in temperature and in magnetic field. The broadening effect may be understood due to the substitution of non-magnetic Ti ions at Mn site which leads to the destruction of Mn^{3+}–O^{2-}–Mn^{4+} network replaced by Mn^{3+}–O^{2-}–Ti^{4+} network [6, 8].

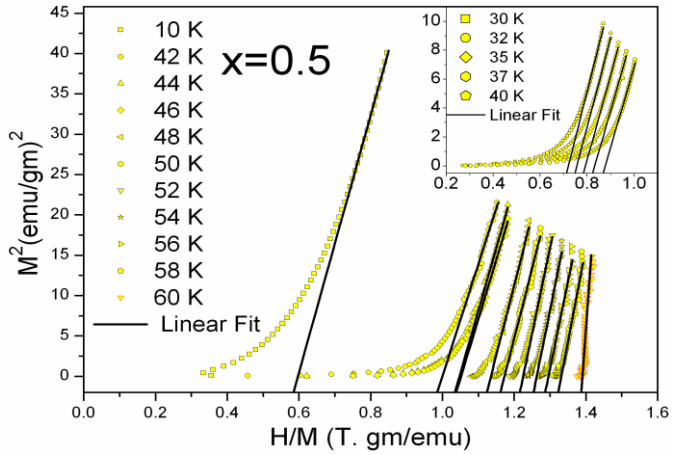

Fig. 5 M^2 vs. H/M (Arrott plots) is displayed at constant temperatures. Inset we display M^2vs. H/M (Arrott plots) at constant temperature measured up to 2.5T. Solid lines are linear fits to the experimental data.

In Fig.6 we show electrical resistivity (ρ) vs. temperature (T) at H=0 and 5T for the studied sample. The application of magnetic field (5T) has no effect on resistivity, since both the resistivity data overlap on one another as shown in Fig.6 with different scales. The sample exhibit semiconducting nature measured throughout the temperature range (180 K < T < 300 K) without any phase transition. The resistivity measurements below 180 K was not possible due to the instrumental limitation as ρ>>1MΩ. This robust insulating behavior indicates the localization (ascribed to $6s^2$ lone pair of Bi^{3+}) of the charge carriers which is common in Bi based samples. However, the substitution of Ti^{4+} at Mn sites could not produce metallic behavior in the sample [6, 8].

The electrical transport of the charge carriers in the sample exhibiting semiconducting nature is generally governed by Variable Range Hopping (VRH) mechanism [6, 8, 10]. It is widely believed that these charge carriers form small polarons connected to local Jahn-Teller (JT) distortions [12] which facilitate the transport by hopping.

The electrical resistivity arising from hopping mechanism follows Arrhenius like equation [6, 8] given by,

$$\rho(T) = \rho_0(T)\exp(T_0/T)^q \quad (1)$$

Where T_0 is a characteristic VRH temperature and characteristic exponent q=1, ¼ and ½ for hopping over the nearest sites (NSH), Mott's VRH and Shklovskii-Efros (SE-VRH) mechanisms respectively [5, 8].

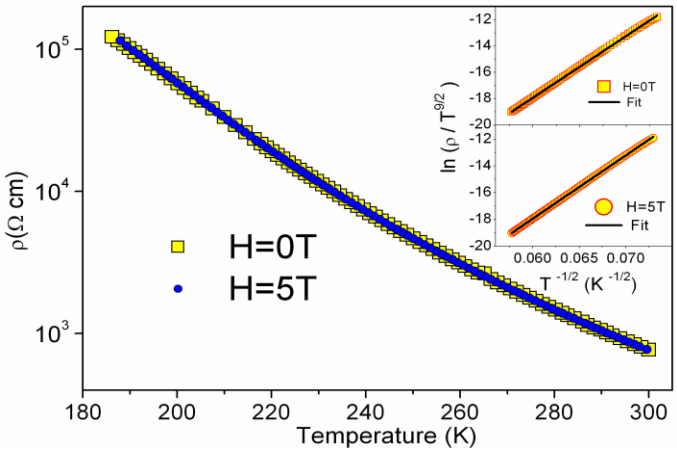

Fig. 6 Resistivity (Ωcm) vs. Temperature (K) at applied magnetic field 0T and 5T for the sample. Inset ln ($\rho/T^{9/2}$) vs. $T^{-1/2}$ ($K^{-1/2}$) with linear fitting is displayed for both at 0T and 5T.

The later mechanism is being used to analyze the transport behavior in the sample which depends on the Coulomb Gap (CG) in the vicinity of the localized density of states (DOS). It is further understood that this model well describes the transport mechanism in the sample, where the DOS near Femi energy (E_F) is not constant but vanishes linearly with energy [5, 8]. This vanishing DOS, results in the temperature dependence of resistivity which still describes eq (1) but with q=½ in all dimensions. In SE-VRH regime the pre-factor ρ_0 (T) can be written as ρ_0 (T) $=CT^n$ in eq. (1), where C is constant and n is 9/2 or 5/2. The values 9/2 or 5/2 assigned for 'n' depends on wave function of the localized charge carriers [8]. Then eq. (1) in logarithmic form is plotted as ln (ρ/T^n) vs. T^{-q}, where n and q are chosen to be 9/2 and ½ respectively. By linear fits for these plots as shown in inset of Fig.6 yields the values of T_0 $=2.239\times10^5$ K for H=0T and 2.226×10^5 K for H=5T. It can be observed that the value of T_0 varies only at second decimal point with the application of magnetic field which is influenced by the width (Δ) of CG [8]. The Δ is found to be 0.556 eV for H=0T and 0.554 eV for H=5T. These values are estimated using the equation, $\Delta=K_B(T_0T_V)^{½}$ [8], where T_V (~186 K) is onset of VRH temperature. The obtained values infer that application of the magnetic field has no effect in reducing the 'Δ' between the Mn hopping sites.

This article has been accepted for publication in a future issue of this journal, but has not been fully edited. Content may change prior to final publication. Citation information: DOI 10.1109/TMAG.2015.2433394, IEEE Transactions on Magnetics

We have also verified the values chosen for 'n' and 'q' by presenting the local activation energy (E_{loc}) model. The E_{loc}= d(lnρ)/d(1/ K_BT) [5, 8] as shown in Fig.6 for both H=0T and 5T nearly matches and found to increase with temperatures. Further from E_{loc} and eq (1) we get,

$$ln\,[E_{loc}/(K_BT)+n] = ln\,q + q\,lnT_0 + q\,ln(1/T) \quad (2)$$

If T_0 is independent of temperature then 'n' varies within some arbitrary interval and 'q' can be obtained from the slope by fitting ln [E_{loc}/(K_BT)+9/2] vs. ln (1/T) as shown inset of Fig.7. The obtained best fit value of q ≈ 0.51 suggests that assigned value of n=9/2 and the transport of charge carriers via hopping is in good agreement with SE-VRH mechanism [5, 8].

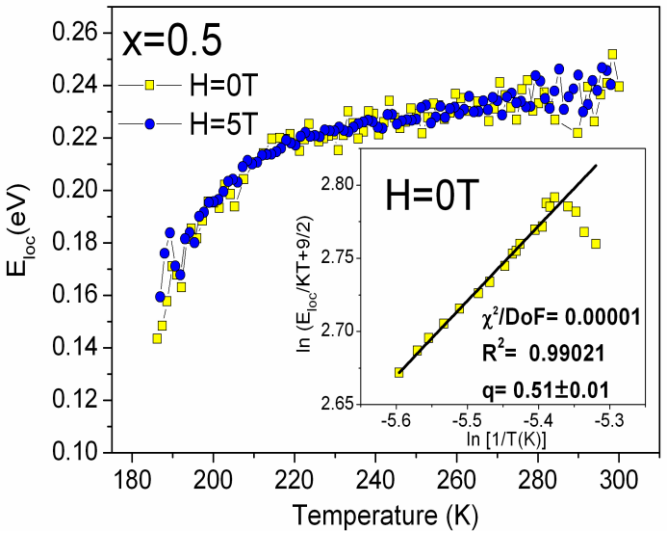

Fig. 7 Local activation energy (E_{loc}) vs. temperature at applied magnetic field 0T and 5T for the sample. Inset ln [E_{loc}/(K_BT)+9/2] vs. ln (1/T) at H=0T with least square fitting (LSF) to find the values of characteristic exponent 'q' is displayed.

IV. Conclusions

In summary, we have reported on magnetic interactions and electronic transport properties in $La_{0.4}Bi_{0.6}Mn_{0.5}Ti_{0.5}O_3$ perovskite manganite. The magnetic properties of the sample indicate the absence of true long range FM interaction due to criticality in their magnetic spin arrangements in temperature region nearby T_C. The exhibited behavior is consistent with the non-magnetic nature of Ti substitution at Mn site. The hopping transport of the charge carriers is due to SE-VRH mechanism which is usually observed for those samples with magnetic inhomogenities and disorder in their local lattice ordering. However the applied magnetic field is also not sufficient to remove this degeneracy in conduction process.

Acknowledgment

This work is supported by Department of Atomic Energy-Board of Research of Nuclear Sciences (**DAE-BRNS**), Govt. of India under DAE-Young Scientist research Award to VD via project sanction No: **2011/20/37P/01/BRNS**. PKV is indebted to DAE-BRNS for SRF fellowship. RLH, DCJ and authors acknowledges Barbara and James Palmer Endowment at the Department of Electrical and Computer Engineering, Iowa State University, USA for XRD, SEM & EDS and magnetization measurements. Authors are grateful to Dr. V. Ganesan, Center director, UGC-DAE CSR, Indore for the experimental facilities and extended support. We concede our thanks to Dr. R Rawat and Mr. Sachin Kumar, MTC lab, UGC-DAE CSR, Indore for resistivity measurements.

References

[1] Gary A. Prinz, "Magneto-electronics applications," J. Magn. Magn. Mater. Vol. 200, pp. 57–68, January 1999.

[2] H. Chiba, T. Atou, and Y. Syono "Magnetic and Electrical Properties of $Bi_{1-x}Sr_xMnO_3$: Hole-Doping Effect on Ferromagnetic Perovskite $BiMnO_3$," J. Solid State Chem., Vol. 132, pp. 139–43, August1997.

[3] Vijaylakshmi Dayal and S. Keshri "Structural and Magnetic properties of $La_{0.67}Ca_{0.33}Mn_{1-x}Fe_xO_3$ (x=0-0.07)," Solid State Commun. Vol. 142, pp. 63-66, April 2007.

[4] L. Joshi, S. Keshri, V. Dayal and N. Rama "Existence of Griffiths phase in $La_{0.67}Ca_{0.33}Mn_{0.99}Fe_{0.07}O_3$," J. Alloys and Compounds, Vol. 479, pp. 879-882, June 2009.

[5] V. Punith Kumar, Vijaylakshmi Dayal, R. L. Hadimani, R. N. Bhowmik and D. C. Jiles, "Magnetic and electrical properties of Ti-substituted lanthanum bismuth manganites," J. Mater. Sci. Vol. 50, pp 3562-3575, May 2015.

[6] Vijaylakshmi Dayal, Punith V. Kumar, "Investigation of electrical resistivity and magnetotransport properties of the $La_{0.67}Ca_{0.33}Mn_{0.99}Fe_{0.01}O_3$ perovskite oxide," Solid State Commun. Vol. 158, pp.70–75, March 2013.

[7] V. Dayal and V. Punith Kumar "Investigation of complex magnetic state in $La_{0.8}Bi_{0.2}MnO_3$,"J. Magn. Magn. Mater. Vol. 361, pp. 212–218, June 2014.

[8] R. Laiho, K.G. Lisunov, E. Lahderanta, J. Salminen, M. A. Shakhov, V. S. Stamov, P. A Petrenko, V. S Zakhvalinskii", Non-universal low-field magnetic scaling and variable-range hopping conductivity as a consequence of disorder in $La_{1-x}Ca_xMn_{1-y}Fe_yO_3$," J. Phys. Chem. Solids, Vol.64, pp.1573–1577, September 2003.

[9] A. K. Pramanik and A. Banerjee, "Critical behavior at paramagnetic to ferromagnetic phase transition in $Pr_{0.5}Sr_{0.5}MnO_3$: A bulk magnetization study," Phys. Rev. B Vol. 79, pp. 214426, June 2009.

[10] Vijaylakshmi Dayal, Punith Kumar V., R. L. Hadimani, and D. C. Jiles, "Evolution of Griffith's phase in $La_{0.4}Bi_{0.6}Mn_{1-x}Ti_xO_3$ perovskite oxide," J. App. Phys, Vol. 115, pp. 17E111-1 to 17E111-3, January 2014.

[11] B. K. Banerjee "On a generalised approach to first and second order magnetic transitions," Phys. Lett. Vol. 12, pp.16-17, September 1964.

[12] H. A. Jahn, E. Teller "Stability of Polyatomic Molecules in Degenerate Electronic States. I. Orbital Degeneracy," Proc. Royal Soc. A , vol. 161, pp. 220-235, July 1937.